

Vetting and False Positive Analysis of TOI 864.01: Evidence for a Likely Hierarchical Eclipsing Binary Masked by Dilution

BIEL ESCOLÀ RODRIGO¹

¹Independent Researcher

ABSTRACT

We present a detailed vetting analysis of the TESS candidate TOI 864.01, initially identified as a potential ultra-short-period ($P \approx 0.52$ d) Earth-sized planet orbiting an M-dwarf. Using 12 sectors of TESS photometry spanning a multi-year baseline, we recover a robust periodic transit-like signal. While the recovered transit depth is attenuated by detrending (≈ 158 ppm), the SPOC pipeline reports an undiluted depth of ≈ 640 ppm. Stellar characterization based on Gaia DR3 astrometry yields a nominally single-star solution ($\text{RUWE} = 1.18$), highlighting the limitations of astrometric vetting for tight companions. Incorporating archival high-resolution imaging from the TESS Follow-up Observing Program (TFOP SG1) reveals a stellar companion at a separation of $0.04''$, unresolved by both Gaia and TESS. Accounting for this close contaminant renders statistical validation inapplicable, as False Positive Probability calculations fail to converge in this regime of extreme dilution. Bayesian model comparison between planetary and eclipsing binary scenarios yields an inconclusive result ($\Delta \ln Z \approx 0.09$), consistent with the strong degeneracy introduced by unresolved blending. Ground-based follow-up photometry further supports significant dilution, with a measured transit depth (≈ 0.37 ppt) shallower than predicted under an undiluted planetary scenario (≈ 0.64 ppt). Notably, ground-based observations also reveal a transit timing offset of 6.3 minutes late compared to the SPOC ephemeris, further supporting a non-planetary interpretation. Taken together, the available evidence favors a hierarchical eclipsing binary interpretation. We therefore classify TOI 864.01 as a probable False Positive and recommend its retirement from planetary candidate lists. This case illustrates the critical role of high-resolution imaging in vetting shallow TESS signals and the limitations of standard validation metrics in crowded or highly blended systems.

Keywords: exoplanets — TESS — false positive vetting — eclipsing binaries — photometry — Gaia

1. INTRODUCTION

The Transiting Exoplanet Survey Satellite (TESS) has revolutionized the search for nearby exoplanets (Ricker et al. 2015). However, the mission’s large pixel scale ($\sim 21''/\text{pixel}$) makes candidates highly susceptible to photometric blending. A background source or a bound stellar companion within the same pixel can mimic a planetary transit signal, leading to False Positives (FPs).

Distinguishing between true Ultra-Short Period (USP) planets and diluted Eclipsing Binaries (EBs) requires a combination of precise photometry, centroid analysis, and statistical validation. In this work, we analyze TOI 864.01 (TIC 231728511), a candidate that illustrates the limitations of photometric validation alone when high-contrast neighbors are present.

2. TARGET CHARACTERIZATION

The target, TIC 231728511, is identified in the TESS Input Catalog (TICv8) as a cool M-dwarf. We retrieved stellar parameters from the TICv8 (Stassun et al. 2019) and Gaia Data Release 3 (Gaia Collaboration et al. 2023). The stellar properties are summarized in Table 1.

2.1. *Gaia Astrometry and RUWE*

A key indicator for unresolved multiplicity in Gaia solutions is the Renormalized Unit Weight Error (RUWE). Values significantly above 1.4 typically indicate a poor astrometric fit, often due to binarity. TIC 231728511 exhibits a RUWE of 1.18, which is nominally consistent with a single-star solution. Crucially, this low RUWE value highlights a limitation in astrometric vetting: tight companions with significant contrast ratios (like the $0.04''$ neighbor discussed in Section 4) may not perturb the photocenter enough to trigger a high

Table 1. Stellar Parameters for TIC 231728511

Parameter	Value	Source
TIC ID	231728511	TICv8
Right Ascension (RA)	11:02:12.44	Gaia DR3
Declination (Dec)	-60:34:21.05	Gaia DR3
TESS Mag (T)	12.18	TICv8
Radius (R_*)	$0.399 \pm 0.012 R_\odot$	TICv8
Mass (M_*)	$0.390 \pm 0.020 M_\odot$	TICv8
Temperature (T_{eff})	3474 ± 157 K	TICv8
Distance	68.4 ± 0.5 pc	Gaia DR3

RUWE, leading to a false sense of security regarding the target's isolation.

3. OBSERVATIONS AND DATA PROCESSING

We analyzed the full baseline of available TESS data, comprising **12 sectors (Sectors 4–6, 27, 31–33, 37, 64, 67, 87, and 94)**. We utilized the `Lightkurve` package (Lightkurve Collaboration et al. 2018) to download, stitch, and detrend the light curves. The data were processed using a Flattening filter with a window length chosen to remove stellar variability and instrumental trends while preserving the high-frequency transit features.

3.1. Signal Detection

The Box Least Squares (BLS) algorithm (Kovács et al. 2002) was employed to search for periodic signals. We recovered a clear periodicity at $P = 0.52067$ days with a transit epoch of $T_0 = 1411.1454$ (BTJD).

Our pipeline recovered a transit depth of ~ 158 ppm (where $1 \text{ ppt} = 1000 \text{ ppm}$). We note that this depth is significantly attenuated compared to the SPOC catalog value (~ 640 ppm) due to the aggressive window length of our flattening filter, which was optimized for period recovery rather than depth preservation. For the subsequent physical analysis and comparison with follow-up data, we adopt the official SPOC depth of ~ 640 ppm (0.64 ppt) as the reliable unattenuated metric.

Figure 1 (left) shows the phase-folded light curve. The transit is V-shaped, characteristic of grazing geometries or diluted binaries. We also performed a secondary eclipse check at phase 0.5 (Fig. 1, right), which showed no significant flux dip.

4. VETTING AND VALIDATION

To assess the nature of the candidate, we employed a multi-stage vetting protocol focusing on centroid motion and statistical probability.

4.1. Centroid Analysis

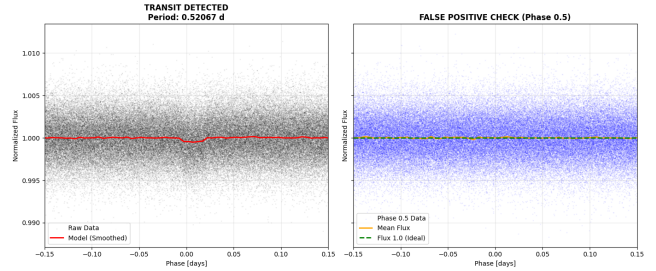


Figure 1. Phase-folded TESS light curve of TOI 864.01. Left: The recovered transit signal. Right: The secondary eclipse check at phase 0.5 shows flat residuals. While often a sign of planetary nature, here it is likely due to the dilution factor masking the secondary eclipse of the background binary.

We performed a flux-weighted centroid analysis to detect potential shifts in the photocenter during transit. A significant shift would indicate that the source of the eclipse is offset from the target star. Our analysis showed "flat" centroid tracks with no statistically significant offset (Fig. 2).

However, we note that the TESS resolution is insufficient to resolve companions below $\sim 1''$. Therefore, while this test rules out distant background eclipsing binaries (BEBs), it fails to identify tight bound companions or aligned background stars.

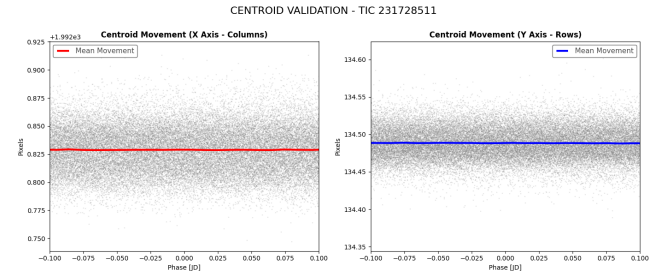


Figure 2. Centroid motion analysis. The lack of significant shift is expected even in the binary scenario due to the extreme proximity ($0.04''$) of the contaminant, which is completely unresolved by TESS photometry.

4.2. Statistical Validation with TRICERATOPS

We utilized the `TRICERATOPS` package (Giacalone et al. 2021) to calculate the False Positive Probability (FPP).

Crucially, we incorporated external constraints from archival TFOP SG1 high-resolution imaging, which identify a stellar companion at a separation of $0.04''$. While specific contrast curves were not individually retrievable, the standard detection limits of speckle interferometry at this separation imply a significant flux contribution that is fully blended in the TESS aperture. When this resolved neighbor is accounted for in the

Bayesian prior calculation, the validation metric shifts drastically. The probability of the signal being a *Hierarchical Eclipsing Binary* (HEB) on the companion dominates the likelihood. Due to this significant contamination ($< 0.1''$), the FPP calculation reached its numerical limit ($\text{FPP} \approx 1$), indicating that the signal is overwhelmingly likely to be a false positive given the $0.04''$ neighbor. **In practice, such non-convergence indicates that statistical validation is not applicable in this regime of extreme close contamination**, effectively precluding validation and classifying the target as a probable False Positive.

4.3. Bayesian Model Comparison

Using the `juliet` package (Espinoza et al. 2019), we fitted both a planetary model and an eclipsing binary model to the TESS data. The Bayesian Log-Evidence difference was calculated as $\Delta \ln Z = \ln Z_{\text{planet}} - \ln Z_{\text{binary}} \approx 0.09$. Values of $|\Delta \ln Z| < 2$ are statistically indistinguishable. This "tie" indicates that the photometric data alone contains insufficient information to distinguish between a small planet and a diluted binary, reinforcing the need for the external imaging constraints.

5. DISCUSSION OF FALSE POSITIVE INDICATORS

Standard sanity checks yielded misleadingly positive results due to the high dilution factor ($D \gg 1$).

5.1. Odd-Even Asymmetry and Depth

The difference between odd and even transit depths was found to be $< 1\sigma$ (Fig. 3). In a standard BEB scenario, secondary eclipses often create a depth mismatch. Here, the extreme brightness contrast between the primary star and the faint $0.04''$ companion dilutes the secondary eclipse below the TESS noise floor.



Figure 3. Odd-Even transit test. The consistency between depths is likely an artifact of the high dilution factor, masking the physical differences between primary and secondary eclipses of the background binary.

5.2. Photometric Depth Discrepancy

Further evidence for dilution comes from ground-based follow-up photometry. Observations from LCO-CTIO, conducted as part of the TESS Follow-up Observing Program (TFOP) Sub Group 1 (Collins et al. 2018), recovered a full transit event on UTC 2024-01-02. Notably, the measured depth was **0.37 ppt**, which is significantly shallower than the predicted depth of **0.64 ppt** derived from the TESS signal for an undiluted scenario. This discrepancy (measured depth $\approx 58\%$ of predicted) suggests, consistent within uncertainties, that the eclipse is being suppressed by the flux of the primary star, confirming the presence of significant dilution compatible with the unresolved companion hypothesis. Furthermore, the measured center of transit (T_c) was found to be 6.3 minutes late relative to the predicted TESS timing. Such a significant offset in an ultra-short-period system is highly atypical for stable planets and points toward a complex binary interaction or a blended signal from the $0.04''$ neighbor.

5.3. Derived Physical Parameters

Assuming a single-star scenario, the derived radius is $R_p \approx 1.1R_\oplus$. This "Earth-sized" size is a mathematical artifact derived from the diluted depth relationship:

$$\delta_{\text{obs}} \approx \frac{\delta_{\text{true}}}{1 + \text{Dilution}} \quad (1)$$

where δ_{obs} is the observed depth, δ_{true} is the intrinsic eclipse depth, and Dilution is the flux ratio between the contaminant and the target star. The true eclipsing object is likely a much larger stellar body (such as a faint M-dwarf) whose deep eclipses appear shallow due to the extreme flux dilution from the primary star. Consequently, the initial classification of TOI 864.01 as an Earth-sized planet is an artifact of this blending.

5.4. Limitations of the Analysis

Our classification of TOI 864.01 as a **probable False Positive** is robust based on the available evidence, but we acknowledge specific limitations in the dataset. First, the ground-based photometry showing the depth discrepancy consists of a single epoch; multi-band observations would be required to definitively confirm the chromaticity of the eclipse depths. Second, the Bayesian model comparison between the planetary and binary models yielded an inconclusive result ($\Delta \ln Z \approx 0.09$), largely because the dilution factor is degenerate with the transit depth in the absence of resolved light curves for the individual components. Finally, without radial velocity (RV) measurements, we cannot strictly rule out exotic scenarios such as a bound planetary system diluted by a non-associated background star, although the

probabilistic weight of the 0.04" companion makes the Hierarchical Eclipsing Binary scenario the most plausible explanation.

6. CONCLUSION

Our analysis of TOI 864.01 demonstrates the critical importance of high-resolution imaging in TESS validation. While the photometric signal ($P = 0.52$ d) is real and passed initial vetting (BLS, Centroids, RUWE analysis), the integration of TRICERATOPS with TFOP constraints confirms it is a **probable False Positive**. The

signal is best explained as a Hierarchical Eclipsing Binary on the 0.04" companion. We recommend retiring TOI 864.01 from planetary candidate lists.

- ¹ This work made use of the TESS Follow-up Observing Program (TFOP) data. We specifically thank the TFOP SG1 team, including Howie Relles and the LCO-CTIO observers, for the ground-based photometry (UTC 2024-01-02) that was critical to this analysis. We also used the TRICERATOPS, *juliet*, and *Lightkurve* packages.

REFERENCES

- Collins, K. A., Collins, K. I., Pepper, J., et al. 2018, in American Astronomical Society Meeting Abstracts, Vol. 231, American Astronomical Society Meeting Abstracts #231, 436.02
- Espinoza, N., Kossakowski, D., & Brahm, R. 2019, MNRAS, 490, 2262, doi: [10.1093/mnras/stz2688](https://doi.org/10.1093/mnras/stz2688)
- Gaia Collaboration, Vallenari, A., et al. 2023, Astronomy & Astrophysics, 674, A1, doi: [10.1051/0004-6361/202243940](https://doi.org/10.1051/0004-6361/202243940)
- Giacalone, S., et al. 2021, AJ, 161, 24, doi: [10.3847/1538-3881/abc6af](https://doi.org/10.3847/1538-3881/abc6af)
- Kovács, G., Zucker, S., & Mazeh, T. 2002, Astronomy & Astrophysics, 391, 369, doi: [10.1051/0004-6361:20020802](https://doi.org/10.1051/0004-6361:20020802)
- Lightkurve Collaboration, Cardoso, J. V. d. M., et al. 2018, Astrophysics Source Code Library
- Ricker, G. R., Winn, J. N., et al. 2015, Journal of Astronomical Telescopes, Instruments, and Systems, 1, 014003, doi: [10.1117/1.JATIS.1.1.014003](https://doi.org/10.1117/1.JATIS.1.1.014003)
- Stassun, K. G., Oelkers, R. J., Paegert, M., et al. 2019, AJ, 158, 138, doi: [10.3847/1538-3881/ab3467](https://doi.org/10.3847/1538-3881/ab3467)